

Multiband superconductors close to a 3D–2D electronic topological transition

G. G. N. Angilella,¹ A. Bianconi,² and R. Pucci¹

¹*Dipartimento di Fisica e Astronomia, Università di Catania,
and Istituto Nazionale per la Fisica della Materia, UdR Catania,
Via S. Sofia, 64, I-95123 Catania, Italy*

²*Dipartimento di Fisica, Università di Roma “La Sapienza”,
and Istituto Nazionale per la Fisica della Materia, UdR Roma “La Sapienza”,
P.le A. Moro, 2, I-00185 Roma, Italy*

(Dated: November 2, 2018)

Within the two-band model of superconductivity, we study the dependence of the critical temperature T_c and of the isotope exponent α in the proximity to an electronic topological transition (ETT). The ETT is associated with a 3D–2D crossover of the Fermi surface of one of the two bands: the σ subband of the diborides. Our results agree with the observed dependence of T_c on Mg content in $A_{1-x}Mg_xB_2$ ($A=Al$ or Sc), where an enhancement of T_c can be interpreted as due to the proximity to a ‘shape resonance’. Moreover we have calculated a possible variation of the isotope effect on the superconducting critical temperature by tuning the chemical potential.

Keywords: MgB_2 ; $Al_{1-x}Mg_xB_2$; $Sc_{1-x}Mg_xB_2$; critical temperature variations; isotope effect; Van Hove singularity; electronic topological transition.

Partial substitution of Al or Sc for Mg in the simple ceramic compound MgB_2 is known to be detrimental for superconductivity^{1,2}. Viewed from the opposite perspective, the *enhancement* of T_c with decreasing Al content $1-x$ in $Al_{1-x}Mg_xB_2$ from ~ 2 K for $x = 0.5$ to $T_c = 39$ K for $x = 1$ has been interpreted as evidence that high- T_c superconductivity in MgB_2 is actually driven by the interband pairing by tuning the chemical potential near a 3D–2D topological transition in one of the subbands^{2,3,4,5}. This tuning enhances the critical temperature by a shape resonance^{6,7,8,9} in the boron superlattice^{5,6,10,11} that is analogous to the Feshbach resonance in ultracold atoms. In $Al_{1-x}Mg_xB_2$, at $x = 0.66$, the overall monotonic dependence of T_c on the Mg content x displays a pronounced kink, that has been related to a 3D–2D crossover of the Fermi surface associated with the boron σ subband⁴. Going from $x = 1$ to $x = 0.5$, the E_{2g} phonon mode energy $\omega_{E_{2g}}$ increases from 70 to 115 meV, while the intra and interband electron-phonon couplings are characterized by unconventional behaviours, reflecting the proximity to such a shape resonance (see Ref. 3 and refs. therein).

A 3D–2D crossover in the σ subband can be described in terms of an electronic topological transition (ETT) of the ‘neck disruption’ kind, according to I. M. Lifshitz’s terminology¹² (see Refs. 13,14 for recent reviews) The proximity to an essentially 2D ETT in the cuprates has been recently connected with the non-monotonic dependence of T_c on doping¹⁵, with the universal dependence of T_c on the in-plane hopping ratio^{15,16}, as well as with the anomalous enhancement of the effect of superconducting fluctuations on several transport properties above T_c ¹⁷.

Here, we consider the effect of the proximity to a 3D–2D ETT on T_c and on the isotope effect of the diborides within a mean-field approach to the two-band model¹⁸. The total observed isotope exponent α in MgB_2 amounts

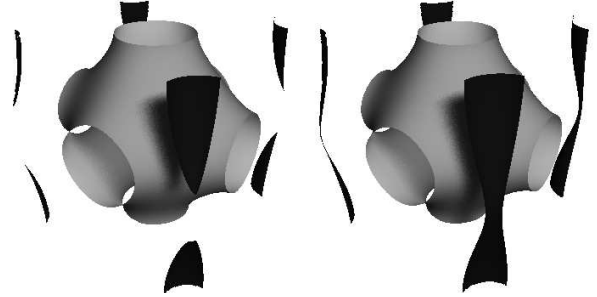


FIG. 1: Typical Fermi surfaces of MgB_2 below (left) and above (right) the ETT. The lighter sheet refers to the π subband, which is characterized by 3D behaviour, and is almost insensitive to the ETT. The darker sheet refers to the σ subband, which is characterized by a 3D (left) to 2D (right) crossover, as the ETT is traversed.

to ~ 0.3 , which is much smaller than the value $\alpha = \frac{1}{2}$ expected for a typical BCS superconductor^{19,20}. This has been interpreted in terms of strong electron-phonon coupling within Migdal-Eliashberg theory²¹, although it has been pointed out that nonadiabatic corrections may be relevant to understand this anomaly²².

The σ and π subbands of the diborides can be described within the tight-binding approximation by a model dispersion relation

$$\xi_{\mathbf{k}}^{(i)} = \epsilon^{(i)} - 2t^{(i)}[\cos k_x + \cos k_y + s^{(i)} \cos k_z] - \mu, \quad (1)$$

where \mathbf{k} is a wavevector in the first Brillouin zone (1BZ), $i = 1, 2$ label the σ and π subbands, respectively, $t^{(i)}$ is the intralayer nearest-neighbour (NN) hopping amplitude, $s^{(i)}$ denotes the ratio of the interlayer to intralayer NN hopping amplitudes, $\epsilon^{(i)}$ is the shift between the centres of the two subbands, and μ is the chemical potential.

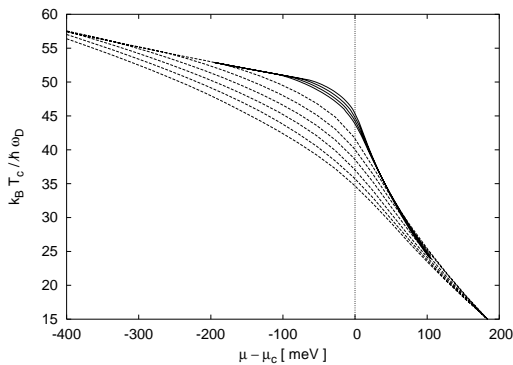


FIG. 2: Thermal energy $k_B T_c$ divided by Debye energy $\hbar\omega_D$ as a function of $\mu - \mu_c$ in the proximity of the ETT (vertical dotted line). Solid lines correspond to $\omega_D = 70 - 115$ meV, while dashed lines correspond to $\omega_D = 200 - 600$ meV (ω_D increases from top to bottom).

A value of $s \approx 1$ can be used to describe a 3D subband, while $s \ll 1$ implies small dispersion along the z direction, and can be used therefore to model a quasi-2D subband. In the following, we will specifically employ the following set of parameters: $t^{(1)} = 0.6$ eV, $s^{(1)} = 0.167$, $\epsilon^{(1)} = 0$, for the σ subband, and $t^{(2)} = 0.9$ eV, $s^{(2)} = 1$, $\epsilon^{(2)} = 2.9$ eV, for the π subband. Fig. 1 shows the typical Fermi surfaces, $\xi_{\mathbf{k}}^{(i)} = 0$, for μ close to the ETT value, $\mu_c = 2.19527$ eV (cf. Ref. 23,24). One recovers a 3D Fermi sheet corresponding to the π subband, almost insensitive to small changes of $\mu \sim \mu_c$, and a tubular Fermi sheet corresponding to the σ subband. As μ increases from below to above μ_c , the latter Fermi sheet undergoes a 3D to 2D ETT.

The densities of states (DOS) $N_i(\xi)$ corresponding to the model dispersion relations, Eqs. (1), have been derived by several authors (see *e.g.* Ref. 25), also including a next-nearest neighbour hopping term, which is here neglected for the sake of simplicity. In the limit $s = 0$, $N_i(\xi)$ can be expressed analytically in terms of elliptic integrals²⁵, and is characterized by a logarithmic, Van Hove singularity at $\xi = 0$. While the π subband has an almost constant DOS around the ETT, due to its 3D character, the DOS corresponding to the σ subband displays a pronounced kink at $\mu = \mu_c$, which is where the Fermi surface changes its topology from 3D to 2D (Fig. 1). To avoid confusion, it should be emphasized that the quasi-Van Hove peak at $\mu = 0$, which is a consequence of the small value of $s^{(1)}$, will not be addressed by the present discussion. The almost singular behaviour at $\mu = 0$ is related to another ETT (corresponding to a change from hole- to particle-like character in the Fermi surface²⁶), whose relevance for the high- T_c cuprates has been emphasized elsewhere (see *e.g.* Refs. 15,16,17, and refs. therein).

Within the two-band model of superconductivity¹⁸, the equation for T_c (essentially, the linearized BCS gap

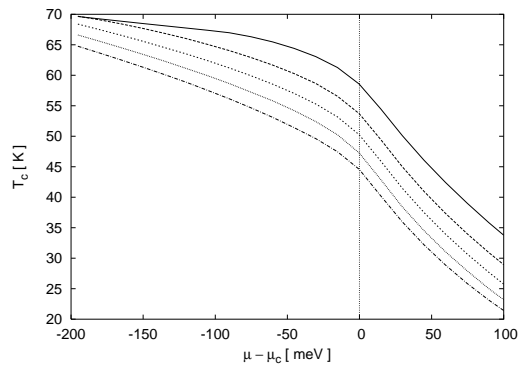


FIG. 3: Critical temperature T_c as a function of $\mu - \mu_c$ in the proximity of the ETT (vertical dotted line). From top to bottom, ω_D increases in the range $100 - 500$ meV at a fixed step of 100 meV, while $V_{12} \simeq 2.09, 1.66, 1.48, 1.37, 1.30$.

equations for a two-band system) reads

$$-1 + V_{11}F_1^c + V_{22}F_2^c + (V_{12}^2 - V_{11}V_{22})F_1^cF_2^c = 0, \quad (2)$$

where V_{ij} are the effective coupling constants between bands i and j ,

$$F_i^c = \int_{-\omega_D}^{\omega_D} d\xi N_i(\xi)\chi_c(\xi), \quad (3)$$

with ω_D denoting the Debye frequency, and $\chi_c(\xi) = (2\xi)^{-1} \tanh(\beta_c \xi/2)$ the pairing susceptibility at the inverse critical temperature $\beta_c = (k_B T_c)^{-1}$. In the absence of interband coupling ($V_{12} = 0$), Eq. (2) factorizes into two equations, and the critical temperature is then the larger onset temperature of superconductivity in each band¹⁸. In order to describe the superconducting diborides via the two-band model, a nonzero value of the interband coupling is therefore important to guarantee two separate gaps, while retaining a single T_c , as evidenced by first-principle calculations²⁷ and observed *e.g.* by point contact spectroscopy²⁸.

We started by numerically evaluating T_c within the two-band model of Eq. (2), as a function of the proximity to the ETT, $\mu - \mu_c$. We employed $V_{11} = 0.2$, $V_{22} = 0.1$, $V_{12} = 2$, while $\omega_D = 70 - 115$ meV (see Ref. 3 and refs. therein). Within a rigid band approximation, a change in the Al/Mg content in $\text{Al}_{1-x}\text{Mg}_x\text{B}_2$ is here parametrized by a change in the chemical potential μ . The actual relation between x and μ is expected to be nonlinear, and has been studied to some extent in Ref. 4. Therefore, we have neglected an explicit dependence of the coupling constants and of the Debye frequency on μ , which may be in principle derived by combining the results of Refs. 4 and 3. However, we do not expect that our results would be changed much, at least qualitatively. Our results are therefore in agreement with Fig. 1 of Ref. 4, showing the experimental variation of T_c in $\text{Al}_{1-x}\text{Mg}_x\text{B}_2$ as a function of Mg content x . In particular, we find a monotonic increase of T_c when the ETT is traversed so that the σ subband undergoes a 3D to 2D crossover. Exactly at the

ETT, $T_c = T_c(\mu)$ is characterized by a shoulder, which corresponds to the kink at $x = 0.66$ in the experimental $T_c = T_c(x)$ of Ref. 4.

In order to extract the isotope coefficient $\alpha = (1/2)(\partial \log T_c / \partial \log \omega_D)$, we have evaluated $\partial T_c / \partial \omega_D$ at fixed μ by differentiating Eq. (2) (see *e.g.* Refs. 25,29,30). Specifically, we find downward deviations from the BCS value $\alpha = \frac{1}{2}$, with a minimum at the ETT. Such a minimum is more pronounced for larger values of the Debye frequency ω_D .

This is not surprising, as has been emphasized³¹ in connection with the role of a logarithmic Van Hove singularity for the anomalous isotope effect of the cuprates^{25,32}. A generic feature of a non-constant DOS is that of providing deviations (even divergences, when logarithmic singularities are present) of α from its standard BCS value³¹. This is a consequence of the asymmetry of the DOS, which has to be evaluated at $\xi = \pm \omega_D$ in the expression for α ²⁹. Such an asymmetry is more pronounced in the proximity to an ETT, where the DOS for the σ subband displays a kink.

However, although the proximity to the ETT tends to decrease the value of the isotope exponent α , the model is not able to recover the anomalously low isotope effect observed experimentally in the diborides. This is probably due to the oversimplification of the model, which does not take into account strong-coupling effects²¹, the nonlinear electron-phonon coupling in the E_{2g} mode³³, and, to a less extent, the unconventional doping dependence of the electron-phonon couplings and of the phonon energy⁴.

For the sake of completeness, we have numerically studied T_c as a function of μ around the ETT varying the other relevant parameters, *i.e.* ω_D and V_{12} . Fig. 2 shows the μ -dependence of the dimensional ratio $k_B T_c / \hbar \omega_D$ for fixed $V_{12} = 2$ and increasing $\omega_D = 70 - 115$ meV and $\omega_D = 200 - 600$ meV. One may conclude that the relative enhancement of T_c near the ETT is greater for smaller ω_D . This is to be expected, since in this case the integral in Eq. (3) selects a shorter energy ‘window’ around the Fermi level, thus increasing the importance of the ETT. On the other hand, Fig. 3 shows the μ -dependence of T_c for increasing $\omega_D = 100 - 500$ meV, with decreasing V_{12} , so to keep $T_c(\mu = 2 \text{ eV}) \approx \text{const.}$

In order to compare with the experimental dependence of T_c on Al content x in $\text{Al}_{1-x}\text{Mg}_x\text{B}_2$ ^{4,34}, we can estimate the dependence of effective couplings λ_{ij} ($i, j = 1, 2$) and of the Debye frequency ω_D of the E_{2g} phonon mode on the proximity $\mu - \mu_c$ of the chemical potential from the ETT by combining the results of Refs. 3,4,34, as is shown in Fig. 4. Then, we can estimate the effective coupling constants in Eq. (2) from $\lambda_{ij} = V_{ij} \sqrt{n_i n_j}$, where n_i is the partial DOS associated with the i -th band. Fig. 5 then shows our results for the critical temperature T_c and the isotope coefficient α as a function of $\mu - \mu_c$. Indeed, one finds a steeper dependence of T_c close to the ETT, in qualitative agreement with the experimental results in Al-doped MgB_2 ^{4,34}.

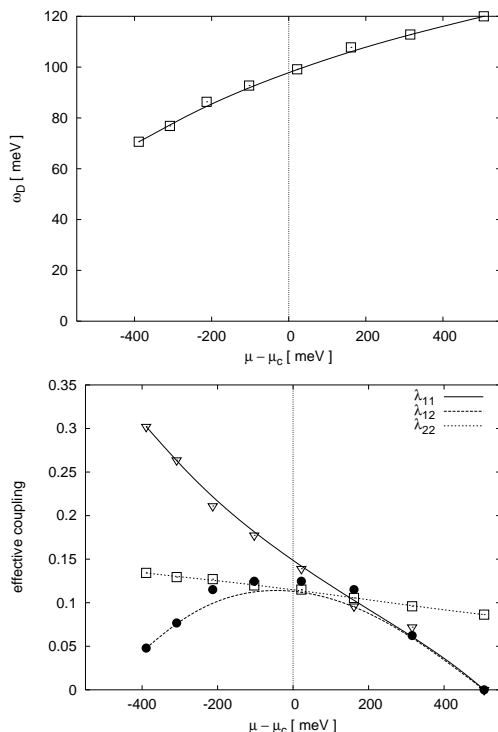


FIG. 4: Upper panel: Dependence of the E_{2g} Debye frequency ω_D as a function of the proximity to the ETT, $\mu - \mu_c$. Lower panel: Dependence of the effective couplings on $\mu - \mu_c$. Lines are guides for the eye.

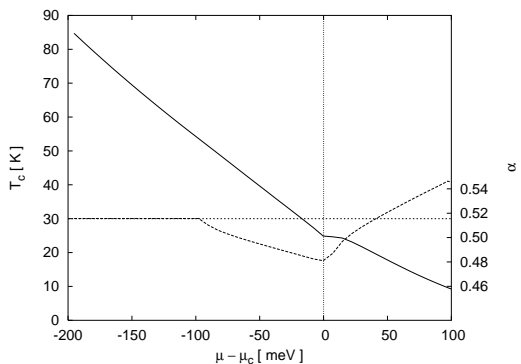


FIG. 5: Critical temperature T_c (solid line, left scale) and isotope exponent α (dashed line, right scale) as a function of chemical potential $\mu - \mu_c$, in the proximity of the ETT (vertical dotted line). Here, we assumed a phenomenological dependence of the Debye frequency ω_D and the effective couplings λ_{ij} on the chemical potential.

In conclusion, within the two-band model of superconductivity, we have studied the effect of the proximity to a 3D–2D crossover (electronic topological transition) on the doping dependence of the critical temperature and of the isotope effect. The proximity to the ETT correctly takes into account, both quantitatively and qualitatively, for the enhancement of T_c as a consequence of a quantum interference effect between the two electronic bands

characterizing the diborides.

Acknowledgments

The authors thank S. Caprara, A. Perali, and A. A. Varlamov for useful discussions.

-
- ¹ J. S. Slusky, N. Rogado, K. A. Regan, M. A. Hayward, P. Khalifah, T. He, K. Inumaru, S. Loureiro, M. K. Haas, and H. W. Zandbergen, *Nature (London)* **410**, 343 (2001).
- ² S. Agrestini, C. Metallo, M. Filippi, L. Simonelli, G. Campi, C. Sanipoli, E. Liarokapis, S. D. Negri, M. Giovannini, A. Saccone, A. Latini, and A. Bianconi, *Phys. Rev. B* **70**, 134514 (2004).
- ³ A. Bussmann-Holder and A. Bianconi, *Phys. Rev. B* **67**, 132509 (2003).
- ⁴ A. Bianconi, S. Agrestini, D. D. Castro, G. Campi, G. Zangari, N. L. Saini, A. Saccone, S. D. Negri, M. Giovannini, G. Profeta, A. Continenza, G. Satta, S. Massidda, A. Cassetta, A. Pifferi, and M. Colapietro, *Phys. Rev. B* **65**, 174515 (2002).
- ⁵ A. Bianconi, *Solid State Commun.* **89**, 933 (1994).
- ⁶ A. Perali, A. Bianconi, A. Lanzara, and N. L. Saini, *Solid State Commun.* **100**, 181 (1996).
- ⁷ A. Bianconi, D. D. Castro, S. Agrestini, G. Campi, N. L. Saini, A. Saccone, S. D. Negri, and M. Giovannini, *J. Phys.: Condens. Matter* **13**, 7383 (2001).
- ⁸ J. M. Blatt and C. J. Thompson, *Phys. Rev. Lett.* **10**, 332 (1963).
- ⁹ C. J. Thompson and J. M. Blatt, *Phys. Lett.* **5**, 6 (1963).
- ¹⁰ A. Valletta, A. Bianconi, A. Perali, and N. L. Saini, *Z. Phys. B* **104**, 707 (1997).
- ¹¹ A. Bianconi, A. Valletta, A. Perali, and N. L. Saini, *Physica C* **296**, 269 (1998).
- ¹² I. M. Lifshitz, *Sov. Phys. JETP* **11**, 1130 (1960), [*Zh. Eksp. Teor. Fiz.* **38**, 1569 (1960)].
- ¹³ A. A. Varlamov, V. S. Egorov, and A. V. Pantsulaya, *Adv. Phys.* **38**, 469 (1989).
- ¹⁴ Ya. M. Blanter, M. I. Kaganov, A. V. Pantsulaya, and A. A. Varlamov, *Phys. Rep.* **245**, 159 (1994).
- ¹⁵ G. G. N. Angilella, E. Piegari, and A. A. Varlamov, *Phys. Rev. B* **66**, 014501 (2002).
- ¹⁶ G. G. N. Angilella, G. Balestrino, P. Cermelli, P. Podio-Guidugli, and A. A. Varlamov, *Eur. Phys. J. B* **26**, 67 (2002).
- ¹⁷ G. G. N. Angilella, R. Pucci, A. A. Varlamov, and F. Onufrieva, *Phys. Rev. B* **67**, 134525 (2003).
- ¹⁸ H. Suhl, B. T. Matthias, and L. R. Walker, *Phys. Rev. Lett.* **3**, 552 (1959).
- ¹⁹ S. L. Bud'ko, G. Lapertot, C. Petrovic, C. E. Cunningham, N. Anderson, and P. C. Canfield, *Phys. Rev. Lett.* **86**, 1877 (2001).
- ²⁰ D. G. Hinks, H. Claus, and J. D. Jorgensen, *Nature (London)* **411**, 457 (2001).
- ²¹ G. A. Ummarino, R. S. Gonnelli, S. Massidda, and A. Bianconi, *Physica C* **407**, 121 (2004).
- ²² E. Cappelluti, S. Ciuchi, C. Grimaldi, L. Pietronero, and S. Strässler, *Phys. Rev. Lett.* **88**, 117003 (2002).
- ²³ J. Kortus, I. I. Mazin, K. D. Belashchenko, V. P. Antropov, and L. L. Boyer, *Phys. Rev. Lett.* **86**, 4656 (2001).
- ²⁴ P. de la Mora, M. Castro, and G. Tavizon, (2004), preprint [cond-mat/0405238](#).
- ²⁵ D. Y. Xing, M. Liu, and C. D. Gong, *Phys. Rev. B* **44**, 12525 (1991).
- ²⁶ A. Ino, C. Kim, M. Nakamura, T. Yoshida, T. Mizokawa, Z. Shen, A. Fujimori, T. Kakeshita, H. Eisaki, and S. Uchida, *Phys. Rev. B* **65**, 094504 (2002).
- ²⁷ A. Y. Liu, I. I. Mazin, and J. Kortus, *Phys. Rev. Lett.* **87**, 087005 (2001).
- ²⁸ R. S. Gonnelli, D. Daghero, G. A. Ummarino, V. A. Stepanov, J. Jun, S. M. Kazakov, and J. Karpinski, *Phys. Rev. Lett.* **89**, 247004 (2002).
- ²⁹ R. Combescot and J. Labbe, *Phys. Rev. B* **38**, 262 (1988).
- ³⁰ J. J. Rodríguez-Núñez and A. A. Schmidt, *Phys. Rev. B* **68**, 224512 (2003).
- ³¹ R. Combescot, *Phys. Rev. Lett.* **68**, 1089 (1992).
- ³² C. C. Tsuei, D. M. Newns, C. C. Chi, and P. C. Pattnaik, *Phys. Rev. Lett.* **65**, 2724 (1990).
- ³³ B. Renker, K. B. Bohnen, R. Heid, D. Ernst, H. Schober, M. Koza, P. Adelman, P. Schweiss, and T. Wolf, *Phys. Rev. Lett.* **88**, 067001 (2002).
- ³⁴ A. Bianconi, S. Agrestini, and A. Bussmann-Holder, *J. Supercond.* **17**, 205 (2004).